

# Organic & Biomolecular Chemistry

Accepted Manuscript



This article can be cited before page numbers have been issued, to do this please use: A. A.G. Fernandes, I. A. Leonarczyk, M. A. B. Ferreira and L. C. Dias, *Org. Biomol. Chem.*, 2019, DOI: 10.1039/C9OB00358D.



This is an Accepted Manuscript, which has been through the Royal Society of Chemistry peer review process and has been accepted for publication.

Accepted Manuscripts are published online shortly after acceptance, before technical editing, formatting and proof reading. Using this free service, authors can make their results available to the community, in citable form, before we publish the edited article. We will replace this Accepted Manuscript with the edited and formatted Advance Article as soon as it is available.

You can find more information about Accepted Manuscripts in the [author guidelines](#).

Please note that technical editing may introduce minor changes to the text and/or graphics, which may alter content. The journal's standard [Terms & Conditions](#) and the ethical guidelines, outlined in our [author and reviewer resource centre](#), still apply. In no event shall the Royal Society of Chemistry be held responsible for any errors or omissions in this Accepted Manuscript or any consequences arising from the use of any information it contains.

## Diastereoselectivity in the Boron Aldol Reaction of $\alpha$ -Alkoxy and $\alpha,\beta$ -Bis-Alkoxy Methyl Ketones

Alessandra A. G. Fernandes,<sup>†</sup> Ives A. Leonarczyk,<sup>††</sup> Marco A. B. Ferreira,<sup>††\*</sup> Luiz Carlos Dias,<sup>†\*</sup>

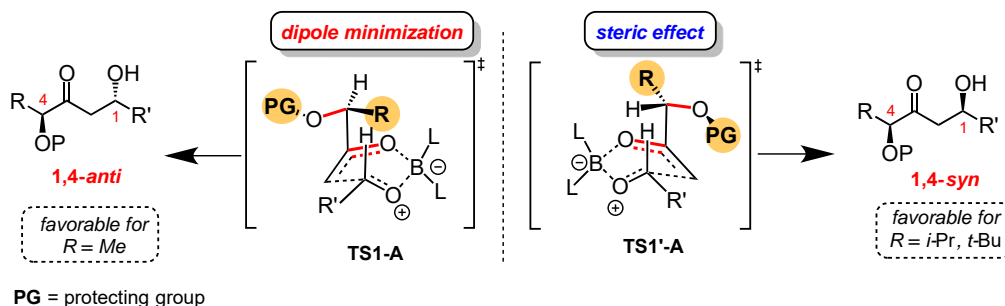
<sup>††</sup> Centre of Excellence for Research in Sustainable Chemistry (CERSusChem), Department of Chemistry, Federal University of São Carlos – 13565-905, Brazil.

<sup>†</sup> Institute of Chemistry, University of Campinas, Campinas –13083-970, Brazil.

**Corresponding Authors** \*Email: marco.ferreira@ufscar.br (M. A. B. Ferreira), ldias@iqm.unicamp.br (L. C. Dias) Tel.: +55-19-35213097.

### ABSTRACT

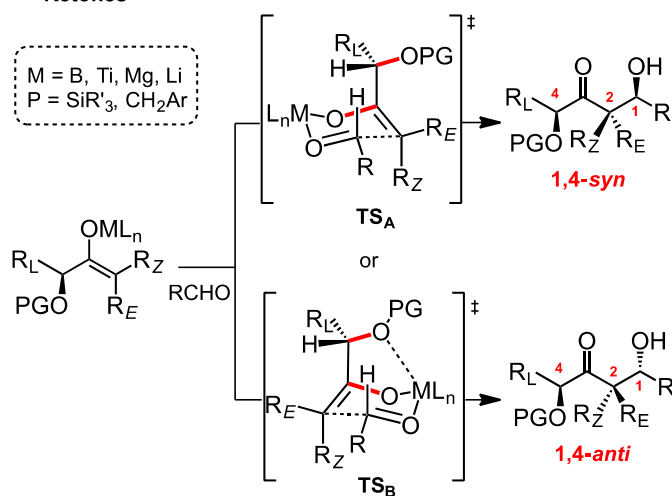
In this work, using DFT calculations, we investigated the 1,4 and 1,5 asymmetric induction presented in boron enolate aldol reactions of  $\alpha$ -alkoxy and  $\alpha,\beta$ -bisalkoxy methyl ketones. We evaluated the steric influence of alkyl substituents at the  $\alpha$  position as well as the stereoelectronic influence of the oxygen protecting groups at the  $\alpha$  and  $\beta$  positions. Theoretical calculations revealed the origins of 1,4 asymmetric induction in terms of the nature of the  $\beta$ -substituent. The synergistic effect between the  $\alpha,\beta$ -*syn* and  $\alpha,\beta$ -*anti*-bisalkoxy stereocenters were elucidated. In the presence of the  $\beta$ -alkoxy center the reaction course goes through the Goodman-Paton 1,5-stereoinduction model, experiencing a minor influence of the  $\alpha$ -alkoxy center.



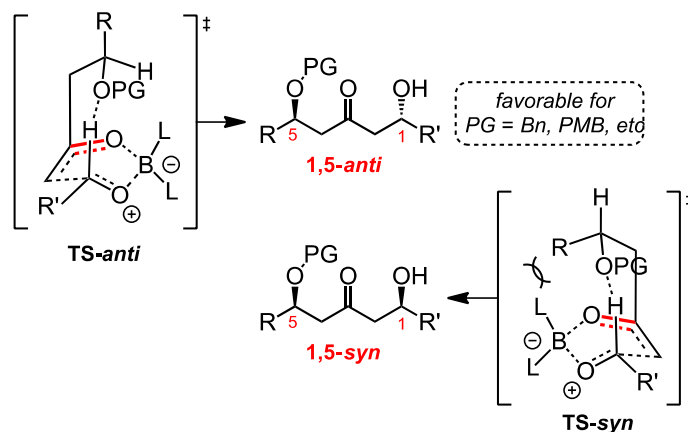
## INTRODUCTION:

The boron-mediated aldol reaction is one of the most versatile and efficient methods for the formation of C-C bonds with regio-, diastereo- and enantioselective control.<sup>1</sup> The application of this reaction is accompanied by the presence of powerful predictive models constructed over the last few decades, allowing its safe application in the preparation of complex molecules, remarkably so for the synthesis of natural products.<sup>1,2</sup> In particular, for metal-mediated aldol reactions of  $\alpha$ -alkoxy ethyl ketones a reasonable set of evidence properly justifies their stereoselectivities.<sup>3</sup> For boron and titanium(IV) enolates it is presumed that the stereoselectivity proceeds through the Zimmerman-Traxler chair-like transition state (Figure 1A, **TS<sub>A</sub>**), in which the both C-O bonds assume an antiperiplanar orientation for dipolar reasons. The R<sub>L</sub>- substituent in the chiral  $\alpha$ -position is arranged outside of the cyclic transition states to minimize 1,3-diaxial interactions, and determines the approach of aldehyde, furnishing the 1,4-*syn* aldol adduct with high diastereoselectivities. The 1,2-relative stereochemistry is determined by the enolate geometry. However, metals like lithium and magnesium are involved in a chelated transition state to afford the opposite diastereoselectivity (Figure 1A, **TS<sub>B</sub>**). For benzyl protecting groups and specific conditions with titanium(IV)<sup>4</sup> the 1,4-*anti* product is observed supposedly through **TS<sub>B</sub>**.

### A. Established Metal-Mediated Aldol Reactions of $\alpha$ -Alkoxy Ethyl Ketones



### B. Goodman-Paton model for Boron-Mediated Aldol Reactions of $\beta$ -alkoxy Methyl Ketones



### C. Boron-Mediated Aldol Reactions of $\alpha$ -Alkoxy and $\alpha,\beta$ -Bisalkoxy Methyl Ketones (*this work*)

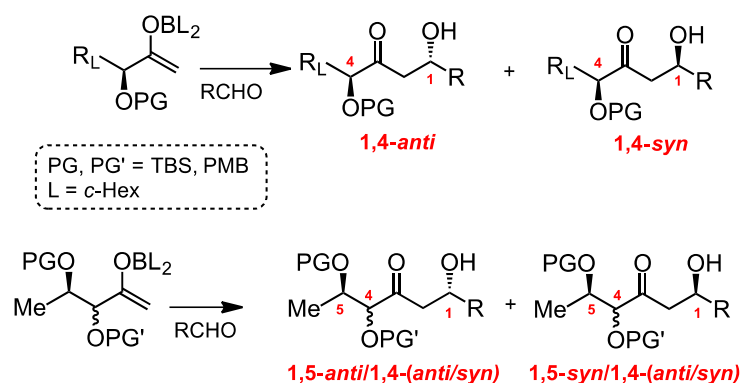
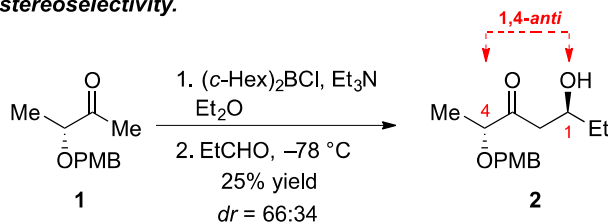
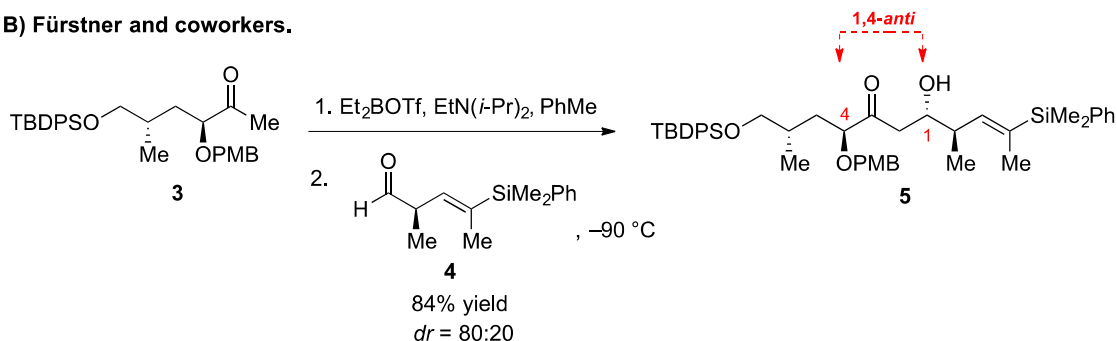
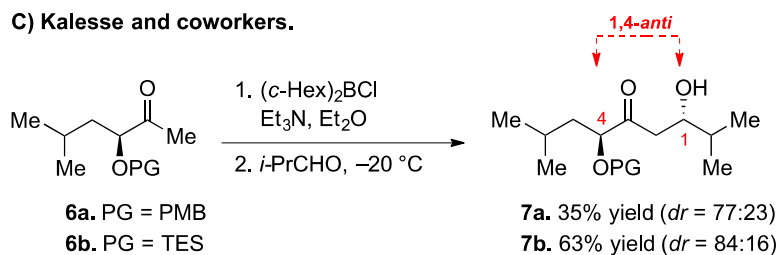
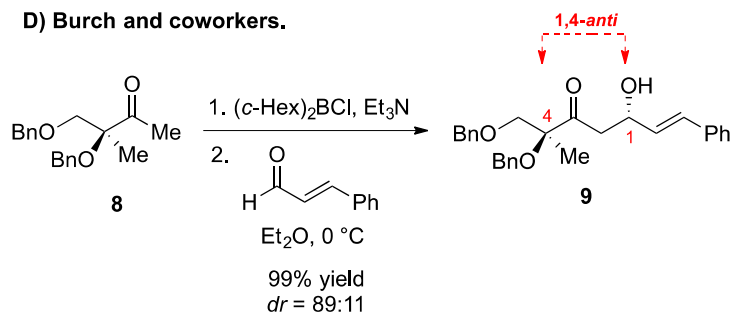


Figure 1. Stereinduction involving  $\alpha$ -alkoxy and  $\alpha,\beta$ -bisalkoxy methyl ketones.

Despite the success of the boron-mediated propionate aldol reactions, the acetyl analogue has proved to be more challenging. These enolborinates preferably react *via* a boat-like transition state in which the 1,3-diaxial interactions are much reduced.<sup>5</sup> In particular, the presence of  $\alpha$ -alkoxy and  $\alpha,\beta$ -bisalkoxy stereocenters in methyl ketones, desirable in the construction of polyhydroxylated natural products, makes its lack of development especially puzzling. The well known Goodman-Paton model describes successfully the remote asymmetric 1,5-induction in boron mediated aldol reactions of  $\beta$ -alkoxy methyl ketones (Figure 1B). These findings showed that the transition state responsible for the stereodeterminant step keeps the  $\beta$ -OPG group towards to the C-H formyl bond and participates in a stabilizing hydrogen bond (H-bond) with the lone pairs of the  $\beta$ -oxygen. The nature of protecting group is critical for the observed high levels of the observed 1,5-*anti* asymmetric induction and involves a puzzling non-covalent interactions balance between the  $\beta$ -substituents, C-H formyl, and boron ligands.<sup>6</sup> Conversely, as unraveled by DFT calculations, except for large protecting groups ( $\text{OSiR}_3$ ,  $\text{OCR}_3$ ) and bulky  $\beta$ -alkyl substituents, the Goodman-Paton model is often predominant over other models to explain the observed stereoinduction.<sup>6,17</sup> However, to date, no successful model has been presented explaining the role of the  $\alpha$ -alkoxy center (Figure 1C).

Some examples involving asymmetric 1,4-induction of  $\alpha$ -alkoxy and  $\alpha,\beta$ -bisalkoxy methyl ketones have been reported. In 1999, Evans and coworkers disclosed the first evidence of a remote 1,4-asymmetric induction in aldol reactions involving boron enolates of  $\alpha$ -alkoxy methyl ketones and aldehydes, as part of the total synthesis of C23-C24 bond of Bryostatin 2 (Figure 2A).<sup>7</sup> Low levels of diastereoselectivities were obtained using  $(c\text{-Hex})_2\text{BCl}$ , although useful levels of 1,4-*syn* and 1,4-*anti* asymmetric induction were observed using chiral boranes. Other more recent contributions were made by Fürstner<sup>8</sup> (Figure 2B), Kalesse<sup>9</sup> (Figure 2C), and Burch<sup>10</sup> (Figure 2D) in the context of total synthesis, similarly showing in the most cases modest 1,4-*anti* diastereoselectivities. It is worth mentioning that synthetically useful results can be achieved using titanium(IV)<sup>11</sup>.

**A) Evans and coworkers. First evidence of 1,4-stereoselectivity.****B) Fürstner and coworkers.****C) Kalesse and coworkers.****D) Burch and coworkers.**

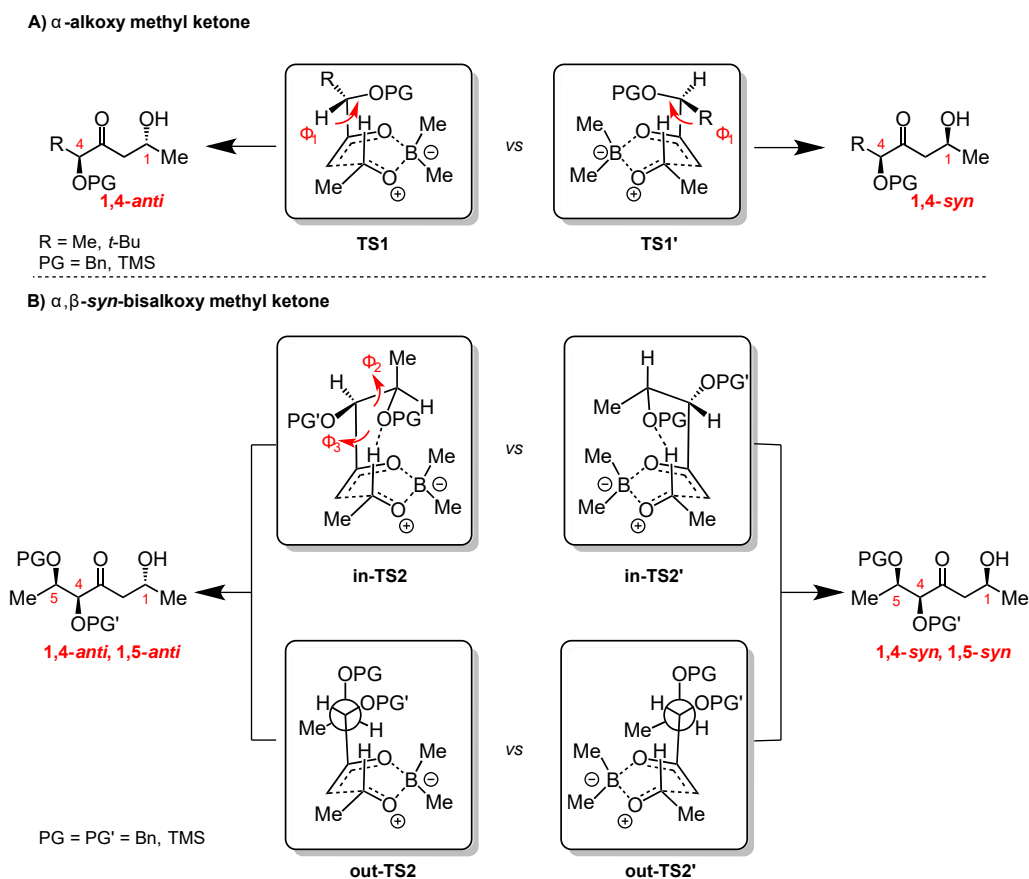
**Figure 2:** Representative examples of 1,4-Asymmetric induction in aldol reactions involving boron enolates of  $\alpha$ -alkoxy methyl ketones.

Due to the lack of detailed studies regarding the factors that influence the 1,4-asymmetric induction in boron-mediated aldol reactions of chiral  $\alpha$ -alkoxy methyl ketones and the synergic effects in  $\alpha,\beta$ -bisalkoxy methyl ketones, we decided to study the influence of the alkyl substituents at the  $\alpha$ -position as well as the nature of the oxygen protecting groups at the  $\alpha$  and  $\beta$  positions using DFT calculations.

## RESULTS AND DISCUSSION

**Computational details.** All DFT calculations were performed with Gaussian 09 using an ultrafine grid.<sup>12</sup> The choice of the level of theory followed previous results from literature,<sup>6</sup> using the B3LYP functional<sup>13</sup> along with 6-31g(d,p) basis set in vacuum for geometry optimization, and the Grimme's D3 dispersion version.<sup>14</sup> We also truncate the boron ligands aiming reduction of computational costs, since previous work shows no relative energy or geometry changes. The structures were visualized using the beta version of CYLview.<sup>15</sup> The frequency calculations (295.15 K at 1 atm) confirmed that the calculated stationary points denote either minima (no imaginary frequency) or transition states (single imaginary frequency) on the potential-energy surface, furnishing also the zero-point vibrational energies, and the thermal and entropic correction from which the Gibbs free energies were determined. To refine the electronic energies, single-point calculations were performed at B3LYP/6-31g(d,p)/IEF-PCM level of theory employing the B3LYP/6-31g(d,p) geometries. The natural bond orbital (NBO) was calculated using NBO 6.0,<sup>16</sup> at B3LYP/6-31g(d,p)/IEF-PCM level of theory. The second-order perturbation analysis (E2PERT=0.05 keyword) estimates the electron delocalization  $LP_O \rightarrow \sigma^*_{C-H}$  associated to the hydrogen bonds stabilization energies.

**Initial considerations.** We considered in our calculations the well known Goodman-Paton model to describe the remote asymmetric 1,5-induction in boron mediated aldol reactions of methyl ketones.<sup>6</sup> Only boat-like transition state geometries were considered, which prevent 1,3-diaxial-type interaction presented in the chair-like conformations. The input geometries for the diastereoisomeric competing transition states **TS1** and **TS1'** were designed considering the rotation of dihedral  $\Phi_1$  generating 3 starting geometries for each diastereoisomers (Scheme 1A). For the  $\alpha,\beta$ -bisalkoxy methyl enolates, additional “**in**” and “**out**” conformers were included, generating at least 9 starting geometries for each diastereoisomer by rotation of dihedral  $\Phi_2$  and  $\Phi_3$ . The Scheme 1B describes the boron enolates of the  $\alpha,\beta$ -*syn*-bisalkoxy methyl ketones. The index “**in**” and “**out**” refers to the relative position of the beta-substituent and the ring in the transition state. We assumed simplifications on the molecular structures by shortening some substituents aiming to reduce the computational costs, but without compromising the quality of the results. Based on the previous literature reports,<sup>6,17</sup> we truncated the boron ligands, replacing *c*-Hex- by Me-. Other simplifications involved the change of more traditional protecting group (PG) substituents TBS- and PMB- by TMS- and Bn-, respectively. Since the diastereoselectivity was mainly controlled by the features of methyl ketones, we choose acetaldehyde in the calculations.



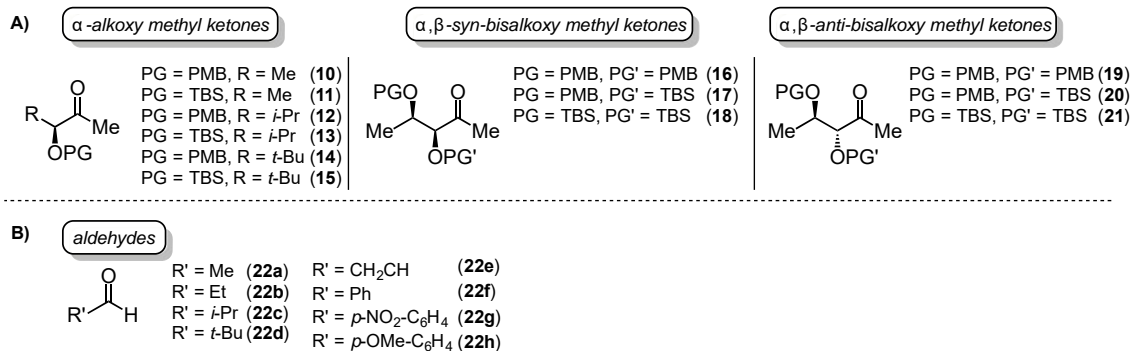
**Scheme 1.** Conformations and substituents considered in the transition states calculations.

Since boron mediated aldol reactions are typically kinetically governed, to evaluate the theoretical diastereoselectivity we computed the equilibrium ratio between diastereoisomer [A]:[B] considering the Boltzmann distribution associated with the Gibbs energies (eqn (1)).<sup>18</sup>  $A_1$  is the most stable transition state conformation among all conformers  $i$  and  $j$ .

$$\frac{[A]}{[B]} = \frac{1 + e^{(\Delta G^\ddagger_{A_1} - \Delta G^\ddagger_{A_2})/RT} + e^{(\Delta G^\ddagger_{A_1} - \Delta G^\ddagger_{A_3})/RT} + \dots + e^{(\Delta G^\ddagger_{A_1} - \Delta G^\ddagger_{A_i})/RT}}{e^{(\Delta G^\ddagger_{A_1} - \Delta G^\ddagger_{B_1})/RT} + e^{(\Delta G^\ddagger_{A_1} - \Delta G^\ddagger_{B_2})/RT} + \dots + e^{(\Delta G^\ddagger_{A_1} - \Delta G^\ddagger_{B_j})/RT}} \quad (1)$$

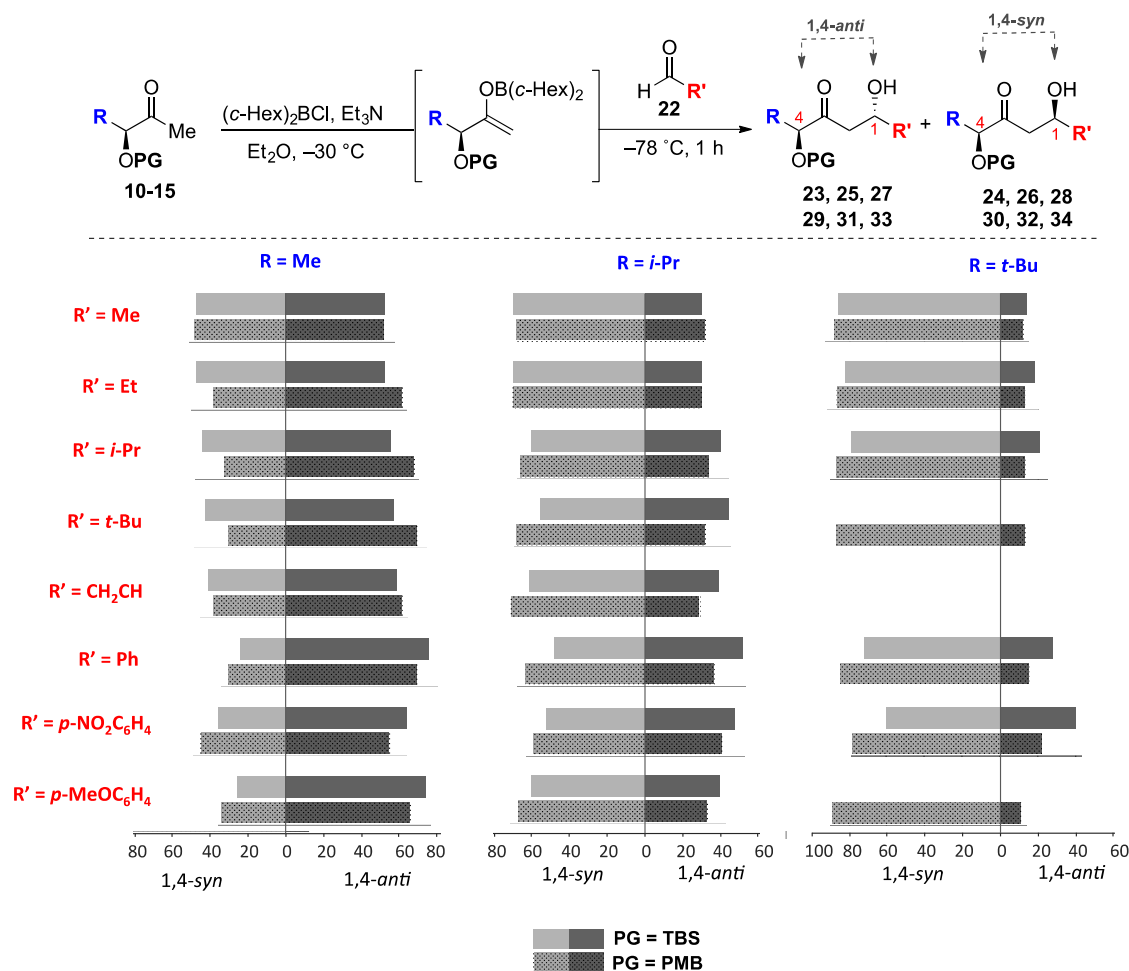
We validated our theoretical models using experimental selectivities obtained from selected reactants (Figure 3). Although we can find some precedents in literature involving asymmetric induction with  $\alpha$ -alkoxy and  $\alpha,\beta$ -bisalkoxy methyl ketones, these findings are generally sparse and the employed ketones are structurally diverse, and/or involve double stereodifferentiation with chiral aldehydes, and therefore do not allow a straightforward rationalization about the importance of stereoelectronic effects. We address this issue by conducting a series of experiments with methyl ketones **10-21** (Figure 3A), from which we systematically evaluate the nature of the protecting groups, and alkyl substituents at  $\alpha$ - and  $\beta$ -positions. The same attention was taken with the set of employed achiral aldehydes

**22a-h** (Figure 3B), presenting a logical variation in their steric and electronic properties. See in the Electronic Supporting Information file all details of these reactions, including preparation of methyl ketones, and proof of stereochemistry of aldol adducts.



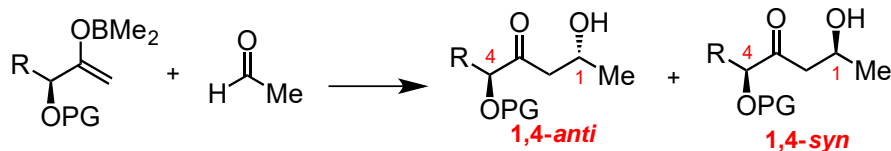
**Figure 3.** **A:** Employed  $\alpha$ -alkoxy and  $\alpha,\beta$ -bisalkoxy methyl ketones. **B:** Employed achiral aldehydes.

**Aldol reactions with  $\alpha$ -alkoxy methyl ketones.** The enolates were prepared *in situ* using (*c*-Hex)<sub>2</sub>BCl, Et<sub>3</sub>N and the corresponding  $\alpha$ -alkoxy methyl ketones **10-15** in Et<sub>2</sub>O at -30 °C. The aldol reactions with the achiral aldehydes **20a-h** provided the corresponding 1,4-*anti* and 1,4-*syn* aldol adducts (Figure 4). Analyzing the results, we noted that the experimental diastereoselectivities were slightly influenced by the nature of protecting groups and aldehydes. The size of the R-substituent in these cases plays a major role in determining the ratio of the products. With R = Me, we observed low to moderate diastereoselectivities favoring the 1,4-*anti* isomer (dr = 52:46 to 76:24). Increasing the bulkiness of R group the aldol reaction increases the sense of induction in favor of the 1,4-*syn* isomer, from dr = 48:52 to 29:71 (R = *i*-Pr) and dr = 11:89 to 28:72 (R = *t*-Bu).



**Figure 4.** Diastereoselectivities in the Boron-Mediated Aldol Reactions of Methyl Ketones **10-15**.

Our theoretical investigation began by locating the transition states for the **1,4-syn** and **1,4-anti** products presented in Scheme 1A. We adopted **TS1** and **TS1'** for **1,4-anti** and **1,4-syn** diastereoisomeric transition structures, respectively. We located the transition states for  $R = \text{Me}$  and  $\text{PG} = \text{Bn}$  (**TS1**<sub>Me,Bn</sub> and **TS1'**<sub>Me,Bn</sub>), for  $R = t\text{-Bu}$  and  $\text{PG} = \text{Bn}$  (**TS1**<sub>t-Bu,Bn</sub> and **TS1'**<sub>t-Bu,Bn</sub>), for  $R = \text{Me}$  and  $\text{PG} = \text{TMS}$  (**TS1**<sub>Me,TMS</sub> and **TS1'**<sub>Me,TMS</sub>), and for  $R = t\text{-Bu}$  and  $\text{PG} = \text{TMS}$  (**TS1**<sub>t-Bu,Bn</sub> and **TS1'**<sub>t-Bu,Bn</sub>). The results of these calculations are summarized in Table 1, and some selected transition structures in Figure 5. Our theoretical calculations (Table 1) produced the same qualitative trends and predicted correctly the major diastereoisomer for 3 cases ( $\text{PG} = \text{Bn}$  for  $R = \text{Me}$ ,  $t\text{-Bu}$ ;  $\text{PG} = \text{TMS}$  for  $R = \text{Me}$ ) but failed for the most hindered system ( $\text{PG} = \text{TMS}$  for  $R = t\text{-Bu}$ ) indicating no theoretical diastereoselectivity (53:47). Probably in this specific case the steric demand of the protecting group and borane ligands would be necessary to better describe the stereodifferentiation.

**Table 1.** Relative Gibbs ( $\Delta\Delta G_{\text{rel}}$ ) energies (kcal mol<sup>-1</sup>), theoretical diastereoselectivities and total dipolar moment for calculated  $\alpha$ -alkoxy methyl ketones.

Enolate	$\Delta\Delta G_{\text{rel}}$ (kcal/mol)	$d r_{\text{theor}}(1,4\text{-anti}:1,4\text{-syn})$ [exp]	Dipole (D)
<b>R = Me, PG = Bn</b>	TS1 <sub>Me,Bn-a</sub> (1,4- <i>anti</i> )	1.4	4.8
	TS1 <sub>Me,Bn-b</sub> (1,4- <i>anti</i> )	1.4	6.0
	TS1 <sub>Me,Bn-c</sub> (1,4- <i>anti</i> )	0.0	96:4 [52:48]
	TS1 <sup>†</sup> <sub>Me,Bn-a</sub> (1,4- <i>syn</i> )	1.3	4.0
<b>R = <i>t</i>-Bu, PG = Bn</b>	TS1 <sub><i>t</i>-Bu,Bn-a</sub> (1,4- <i>anti</i> )	1.3	5.0
	TS1 <sub><i>t</i>-Bu,Bn-b</sub> (1,4- <i>anti</i> )	1.4	3.8
	TS1 <sup>†</sup> <sub><i>t</i>-Bu,Bn-a</sub> (1,4- <i>syn</i> )	7.3	6:94 [21:88]
	TS1 <sup>†</sup> <sub><i>t</i>-Bu,Bn-b</sub> (1,4- <i>syn</i> )	0.0	3.8
<b>R = Me, PG = TMS</b>	TS1 <sub>Me,TMS-a</sub> (1,4- <i>anti</i> )	0.0	5.4
	TS1 <sub>Me,TMS-b</sub> (1,4- <i>anti</i> )	0.6	4.2
	TS1 <sup>†</sup> <sub>Me,TMS-a</sub> (1,4- <i>syn</i> )	2.8	62:38 [53:47]
	TS1 <sup>†</sup> <sub>Me,TMS-b</sub> (1,4- <i>syn</i> )	0.1	4.2
	TS1 <sup>†</sup> <sub>Me,TMS-c</sub> (1,4- <i>syn</i> )	1.6	4.5
<b>R = <i>t</i>-Bu, PG = TMS</b>	TS1 <sub><i>t</i>-Bu,TMS-a</sub> (1,4- <i>anti</i> )	1.3	6.1
	TS1 <sub><i>t</i>-Bu,TMS-b</sub> (1,4- <i>anti</i> )	0.0	4.0
	TS1 <sup>†</sup> <sub><i>t</i>-Bu,TMS-a</sub> (1,4- <i>syn</i> )	0.0	53:47 [14:86]
	TS1 <sup>†</sup> <sub><i>t</i>-Bu,TMS-b</sub> (1,4- <i>syn</i> )	4.4	5.3
	TS1 <sup>†</sup> <sub><i>t</i>-Bu,TMS-c</sub> (1,4- <i>syn</i> )	1.9	4.4

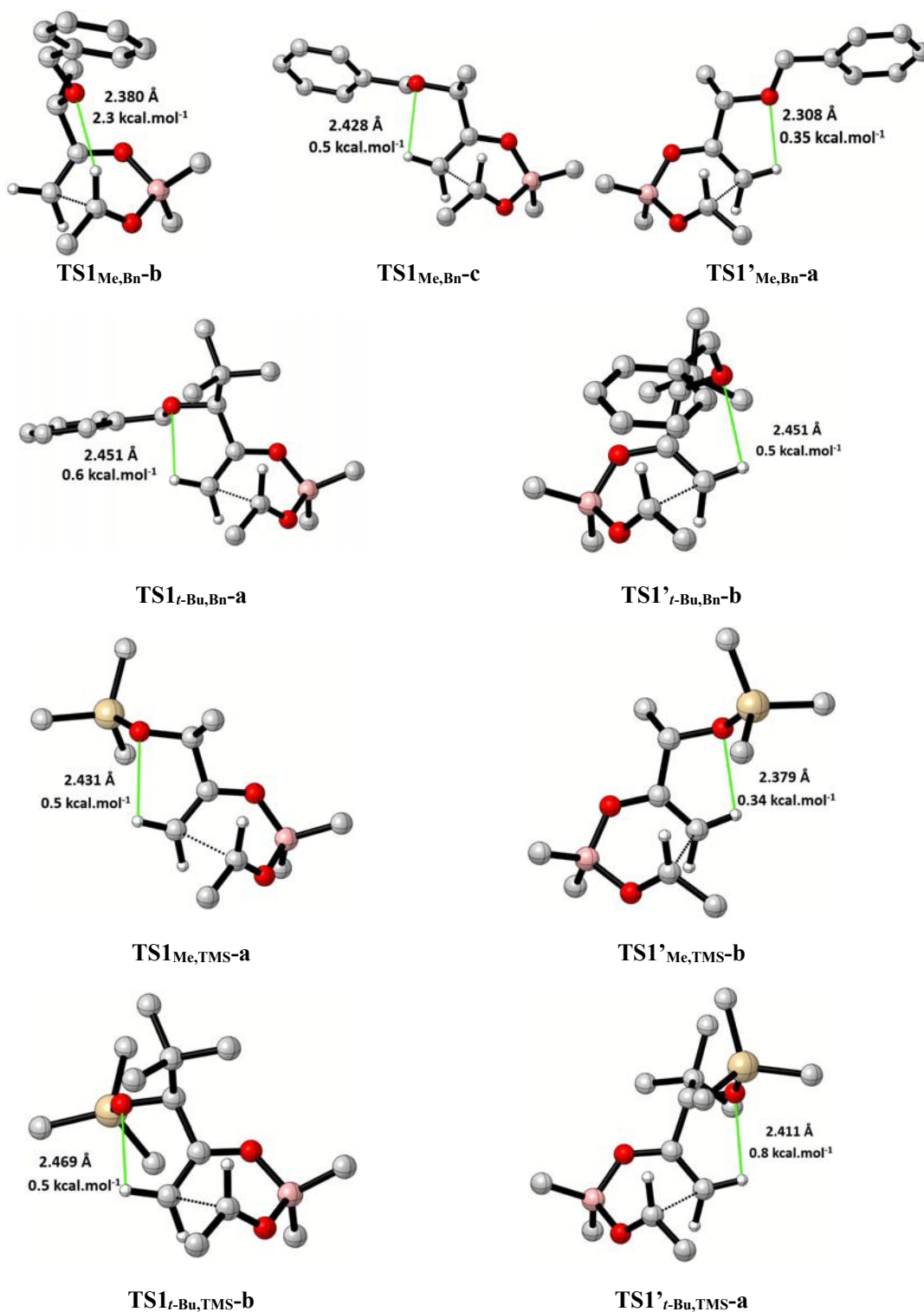


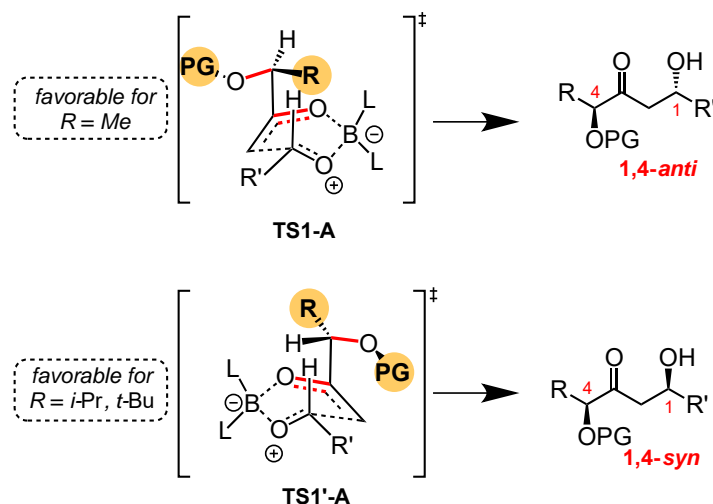
**Figure 5.** Representative transition state structures for calculated  $\alpha$ -alkoxy methyl ketones.

A more in-depth analysis reveals the same non-expected conformations, which present a similar “in” conformation as depicted by the Goodman-Paton model in  $\beta$ -alkoxy methyl ketones transition

structure, and responsible for 1,5-dia stereoinduction.<sup>5</sup> Taking as an example the **TS1<sub>Me,Bn-b</sub>** (Figure 5), this structure keeps the  $\alpha$ -OPG group towards to the C-H formyl bond, and participates in a stabilizing hydrogen bond (H-bond) of 2.3 kcal.mol<sup>-1</sup> between the lone pairs of the  $\alpha$ -oxygen (LP<sub>O1</sub> and LP<sub>O2</sub>) and the  $\sigma^*_{C-H}$  formyl. Nevertheless, this interaction is not enough to stabilize this transition state, being 1.4 kcal.mol<sup>-1</sup> higher in energy than **TS1<sub>Me,Bn-c</sub>**. Similar structures found in other systems also did not present themselves as a minimum in terms of relative energy.

A general analysis of the results showed that the lowest energy diastereoisomeric transition states, conducting to the products 1,4-*anti* and 1,4-*syn*, are those where the both C-O bonds assume an antiperiplanar orientation (Table 1 and Figure 5), very similar to the chair-like chiral  $\alpha$ -OPG ethyl ketone transition states, probably for the same dipolar reasons. The NBO analysis showed in all the cases a very close stabilization energy (0.4-0.8 kcal.mol<sup>-1</sup>) between the LP<sub>O</sub> of  $\alpha$ -OPG and vinyl  $\sigma^*_{C-H}$ , therefore not explaining this energetic preference. Considering the magnitude of the molecular dipole (Table 1), we conclude that dipole minimization plays a major role in the antiperiplanar orientation of C-O bonds, which in most cases the C-O antiperiplanar conformers possess the lowest dipole moments.

Another general observation of lowest energy transition state relates to the orientation of the  $\alpha$ -R group that can be pointed into the transition state ring (Scheme 2). This orientation differs greatly from the established models involving ethyl ketones. This is made possible because the boat type conformation drastically reduces the 1,3-diaxial repulsive interactions. A more detailed analysis also shows that the  $\alpha$ -O-PG and  $\alpha$ -C-R bonds move as far apart as possible each other, preventing severe vicinal repulsive interactions, and in some cases assuming an antiperiplanar conformation. Thus, from the theoretical results, we conclude that the formation of the 1,4-*anti* and 1,4-*syn* diastereoisomers is a consequence of the relative energies between **TS1-A** and **TS1'-A**, respectively, as represented in Scheme 2. The preference between them varies according to the steric nature between R and P - the small group being turned towards the transition state cycle, which is the most crowded position. Consequently, in steric terms, when R = Me we have R <  $\alpha$ -OPG, favoring **TS1-A** over **TS1'-A**, producing the 1,4-*anti* product. In the case of R = *i*-Pr, *t*-Bu, we have that R >  $\alpha$ -OPG since the  $\angle C-(\alpha-C)-O-PG$  dihedral can be adjusted in order to minimize the steric repulsions of the protecting group with the transition state ring. In this situation, the opposite stereoselectivity is expected - 1,4-*syn* product - and **TS1'-A** becomes smaller in energy. By this model, better levels of selectivities depend solely on the difference in steric volume of groups  $\alpha$ -R and  $\alpha$ -OPG, that are not usually as large as the systems studied in this work and present in the literature.



**Scheme 2.** Proposed induction model for  $\alpha$ -alkoxy methyl ketones.

**Aldol reactions with  $\alpha,\beta$ -bisalkoxy methyl ketones.** Once the basis for understanding the diastereoselection of  $\alpha$ -alkoxy methyl ketones was formed, our next incursion sought to unravel the synergism between  $\alpha$ -alkoxy and  $\beta$ -alkoxy stereocenters. We obtained the experimental selectivities for aldol reactions of  $\alpha,\beta$ -*syn* (**16-18**) and  $\alpha,\beta$ -*anti* (**19-21**) bisalkoxy methyl ketones, by first generating the enolates *in situ* using  $(c\text{-Hex})_2\text{BCl}$ ,  $\text{Et}_3\text{N}$  in  $\text{Et}_2\text{O}$  at  $-30\text{ }^\circ\text{C}$ , and the aldol reactions with the achiral aldehydes **20a-h** provided the corresponding aldol adducts (Figure 6).

The high diastereoselectivities ( $\text{dr} > 95:05$ ) for  $\alpha,\beta$ -*syn*-bisalkoxy methyl ketones **16-17** suggest that the PMB protecting group at the  $\beta$  position is critical for the high levels of the observed 1,5-*anti* selectivities. The presence of TBS group at  $\beta$ -position caused an erosion of the selectivity ( $\text{dr} = 59:41$  to  $51:49$ ). Several studies have already been published by Paterson<sup>19</sup>, Evans<sup>20</sup> and Dias<sup>17,21</sup> on aldol reactions of boron enolates of  $\beta$ -alkoxy methyl ketones showing major influence of beta substituents on the 1,5-diastereoselectivity. In the present case the  $\beta$ -position overcomes the 1,4-*syn* sense of induction of  $\alpha$ -position. Intriguingly, the aldol adducts from  $\alpha,\beta$ -*anti*-bisalkoxy methyl ketones (**18-21**) showed lower diastereoselectivities when compared with their  $\alpha,\beta$ -*syn* analogues (**16-18**) showing that the relative stereochemistry between the alkoxy substituents influences the reaction pathway.

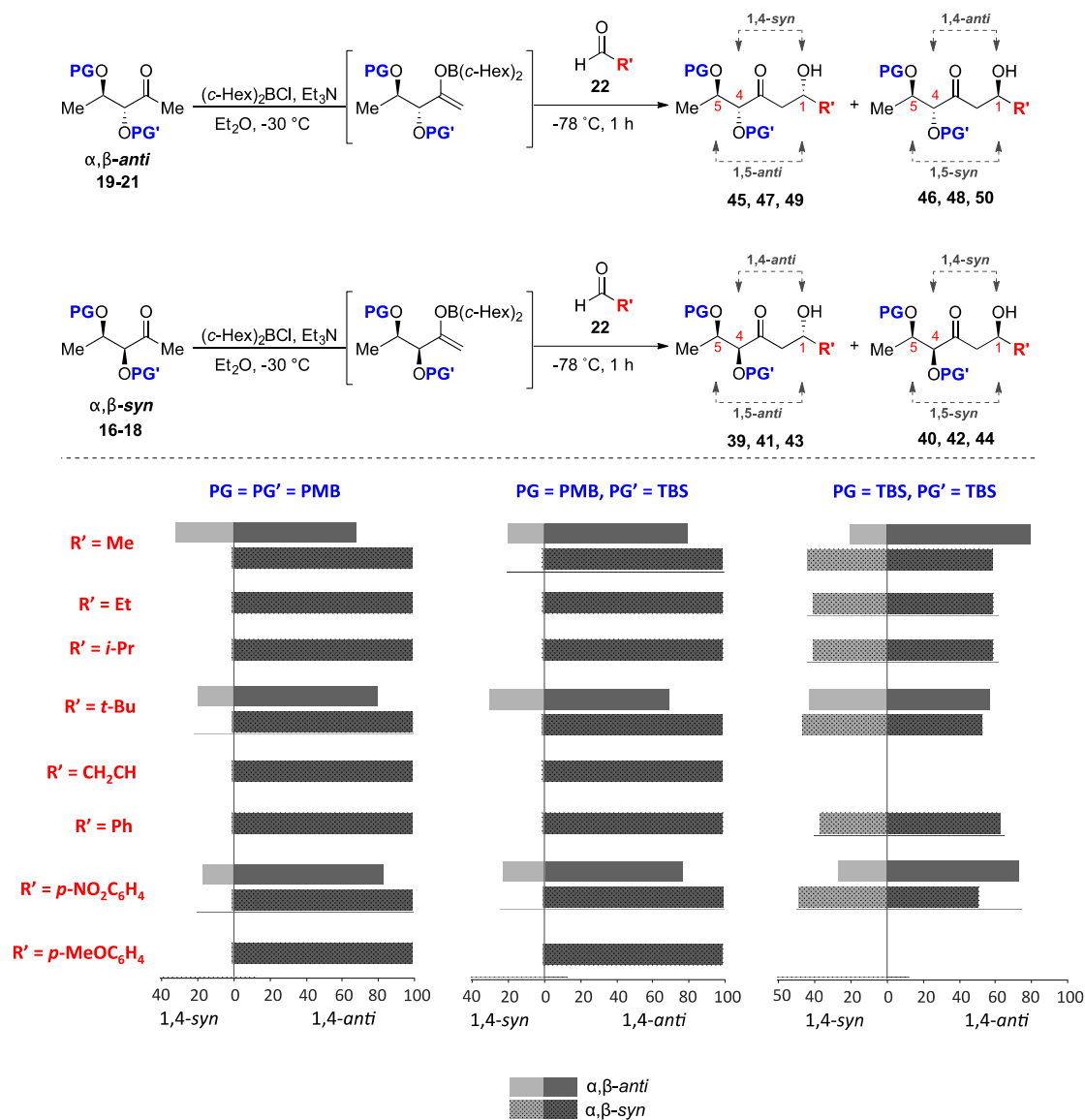
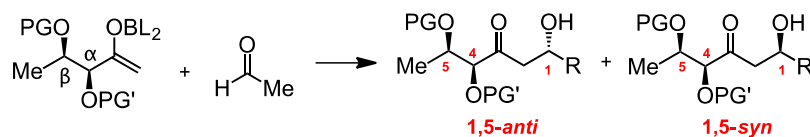


**Figure 6.** Diastereoselectivities in the Boron-Mediated Aldol Reactions of Methyl Ketones 16-21.

Following the protocol outlined in Scheme 1, we mapped all relevant transition states, including  $\alpha,\beta$ -syn-bisalkoxy methyl ketones, with the most important results shown in Table 2 and Figure 7 (for energies of all found diastereoisomeric transition states, see the SI).

**Table 2.** Relative Gibbs ( $\Delta\Delta G_{\text{rel}}$ ) energies ( $\text{kcal mol}^{-1}$ ), and theoretical diastereoselectivities for calculated  $\alpha,\beta$ -*syn*-bisalkoxy methyl ketones.



Enolate		$\Delta\Delta G_{\text{rel}}$ (kcal/mol)	$dr_{\text{theor}}(1,5\text{-anti}:1,5\text{-syn})^*$ [exp]
$\alpha$ -OBn, $\beta$ -OBn- <i>syn</i>	<b>in-TS2</b> <sub>Bn,Bn-<i>syn</i>-c (1,5-<i>anti</i>)</sub>	0.0	>99:5 [>95:05]
	<b>in-TS2'</b> <sub>Bn,Bn-<i>syn</i>-a (1,5-<i>syn</i>)</sub>	1.9	
$\alpha$ -OTMS, $\beta$ -OBn- <i>syn</i>	<b>in-TS2</b> <sub>TMS,Bn-<i>syn</i>-c (1,5-<i>anti</i>)</sub>	0.0	>99:5 [>95:05]
	<b>in-TS2'</b> <sub>TMS,Bn-<i>syn</i>-a (1,5-<i>syn</i>)</sub>	1.9	
$\alpha$ -OTMS, $\beta$ -OTMS- <i>syn</i>	<b>in-TS2</b> <sub>TMS,TMS-<i>syn</i>-c (1,5-<i>anti</i>)</sub>	0.0	74:26 [56:44]
	<b>in-TS2'</b> <sub>TMS,TMS-<i>syn</i>-a (1,5-<i>syn</i>)</sub>	0.3	

\*Determined considering the Boltzmann distribution associated with the Gibbs energies of all observed diastereoisomeric transition states.

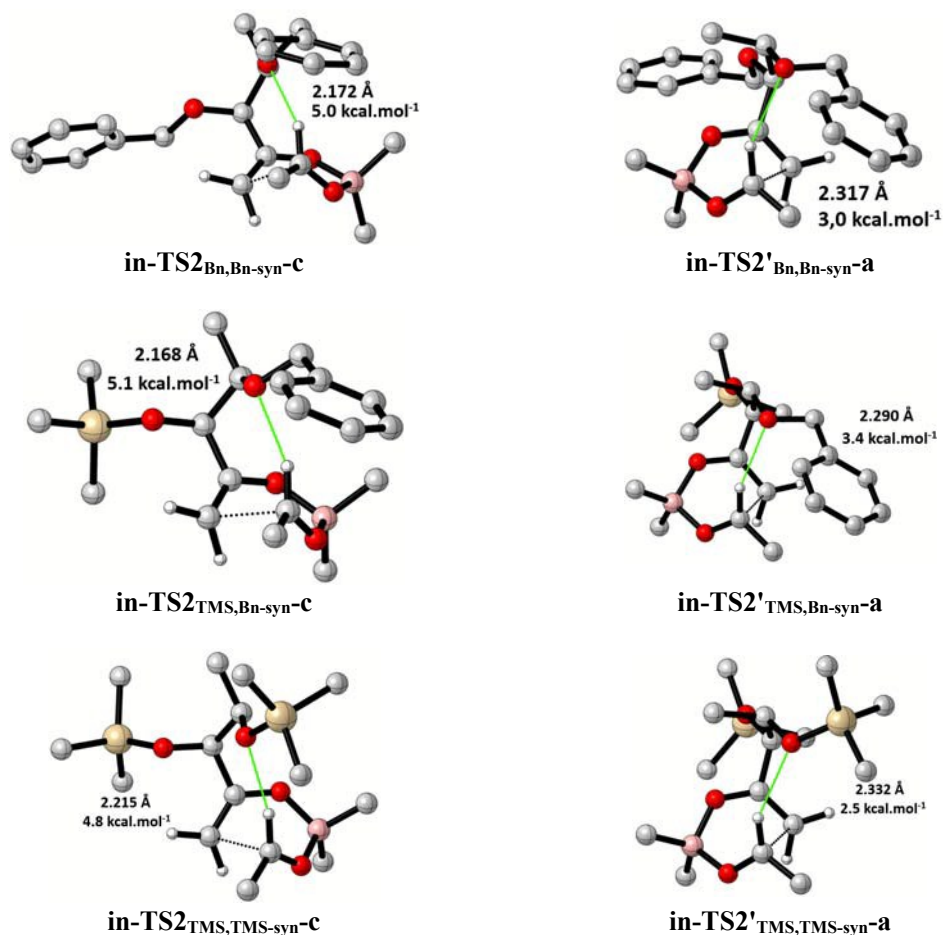
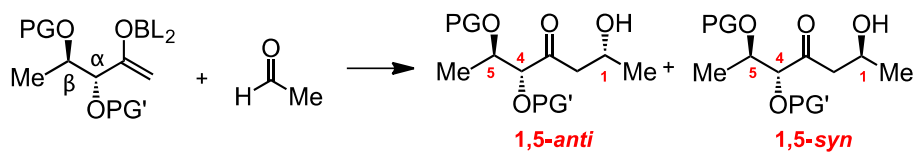


**Figure 7.** Representative calculated transition state geometries for the  $\alpha,\beta$ -*syn*-bisalkoxy methyl ketones.

The results presented in Table 2 show an excellent correlation between the experimental and theoretical diastereoselectivities. A remarkable fact was that for the three investigated ketones -  $\alpha$ -OBn, $\beta$ -OBn-*syn*,  $\alpha$ -OTMS, $\beta$ -OBn-*syn*, and  $\alpha$ -OTMS, $\beta$ -OTMS-*syn* – the transition states **in-TS2** and **in-TS2'** presented the lower energies, providing the 1,5-*anti* and 1,5-*syn* diastereoisomers, respectively. The analysis of their geometries (Figure 7) reveals that these transition states fit with the Goodman-Paton model for 1,5-*anti* selectivity.<sup>5</sup> As discussed before, in this model the lower energy transition states, which provide the 1,5-*anti* and 1,5-*syn* aldol adducts, is organized in such a way that it keeps the  $\alpha$ -OPG group pointing towards to the C-H formyl and participating in a stabilizing H-bond. The preference for the 1,5-*anti* product is given because the lowest energy transition state orientates the  $\beta$ -R group further from the borane ligands than the competitive 1,5-*syn* transition state. In particular, the transition states **in-TS2**<sub>Bn,Bn-*syn*-c</sub> and **in-TS2**<sub>TMS,Bn-*syn*-c</sub> of lowest energies were located for  $\alpha$ -OBn, $\beta$ -OBn-*syn* and  $\alpha$ -OTMS, $\beta$ -OBn-*syn* ketones, respectively, predicting the 1,5-*anti* as the major product. NBO analysis allows for calculation of the energy associated with the stabilizing H-bond of around 5 kcal.mol<sup>-1</sup>. Another feature of these reactions that we could theoretically describe is the non-influence of the  $\alpha$ -alkoxy protecting group in determining diastereoselectivity. This can be appreciated by the same relative energy (1.9 kcal.mol<sup>-1</sup>) between the lowest energy transition states **in-TS2** and **in-TS2'** for  $\alpha$ -OBn, $\beta$ -OBn-*syn* and  $\alpha$ -OTMS, $\beta$ -OBn-*syn* ketones (Table 2). A further insight obtained from the theoretical results has shown that the C-O bonds of the enolate/ $\alpha$ -alkoxy are in an antiperiplanar orientation in both **in-TS2**<sub>Bn,Bn-*syn*-c</sub> and **in-TS2**<sub>TMS,Bn-*syn*-c</sub> which configures a match case in which the 1,5-*anti* induction is reinforced by the  $\alpha$ -alkoxy center. Conversely, in the higher energy transition states **in-TS2'**<sub>Bn,Bn-*syn*-a</sub> and **in-TS2'**<sub>TMS,Bn-*syn*-a</sub>, these same bonds are less favorably oriented, cancelling out the stabilizing effect of dipole minimization. In contrast, the loss of diastereoselectivity for the  $\alpha$ -OTMS, $\beta$ -OTMS-*syn* ketone can be understood in a manner analogous to that already seen in the Goodman-Paton model, where  $\beta$ -OSiR<sub>3</sub> protecting groups exert severe steric repulsion with the ring and borane ligands, in both "in" transition states, generating the drop in the diastereoselectivity. We were able to capture this effect, as can be seen, in the energy difference of 0.3 kcal.mol<sup>-1</sup> between **in-TS2**<sub>TMS,TMS-*syn*-c</sub> and **in-TS2'**<sub>TMS,TMS-*syn*-a</sub>. The model depicted in Scheme 3 summarizes all previous observations regarding the synergistic effect between the  $\alpha,\beta$ -*syn*-bisalkoxy stereocenters.

Our next step involved the study of  $\alpha,\beta$ -*anti*-bisalkoxy methyl ketones, aiming to find the origins for the drop of 1,5-*anti* diastereoselectivity (Figure 6). The most important results can be seen in Table 3 and Figure 8 (for energies of all found diastereoisomeric transition states, see the SI).

**Table 3.** Relative Gibbs ( $\Delta\Delta G_{\text{rel}}$ ) energies ( $\text{kcal mol}^{-1}$ ), and theoretical diastereoselectivities for calculated  $\alpha,\beta$ -*anti*-bisalkoxy methyl ketones.



Enolate		$\Delta\Delta G_{\text{rel}}$ ( $\text{kcal/mol}$ )	$d r_{\text{theor}}(1,5\text{-anti}:1,5\text{-syn})^*$ [exp]
$\alpha$ -OBn, $\beta$ -OBn- <i>anti</i>	<b>in-TS3<sub>Bn,Bn-anti-c</sub> (1,5-<i>anti</i>)</b>	0.0	77:23 [68:32]
	<b>in-TS3'<sub>Bn,Bn-anti-b</sub> (1,5-<i>syn</i>)</b>	0.6	
$\alpha$ -OTMS, $\beta$ -OBn- <i>anti</i>	<b>in-TS3<sub>TMS,Bn-anti-b</sub> (1,5-<i>anti</i>)</b>	0.0	70:30 [80:20]
	<b>in-TS3'<sub>TMS,Bn-anti-a</sub> (1,5-<i>syn</i>)</b>	0.7	

\*Determined considering the Boltzmann distribution associated with the Gibbs energies of all observed diastereoisomeric transition states.

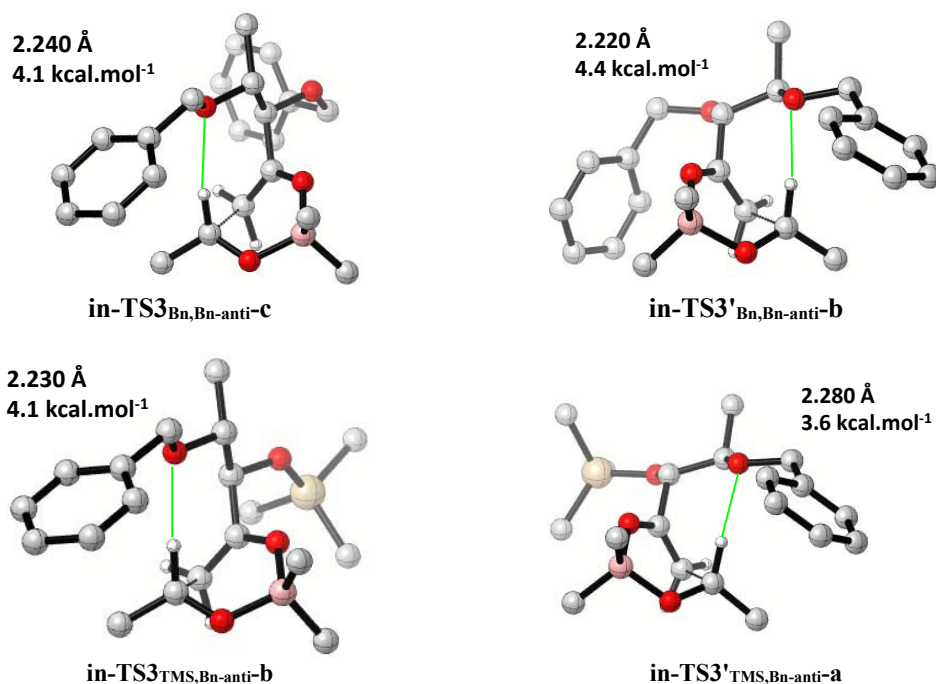
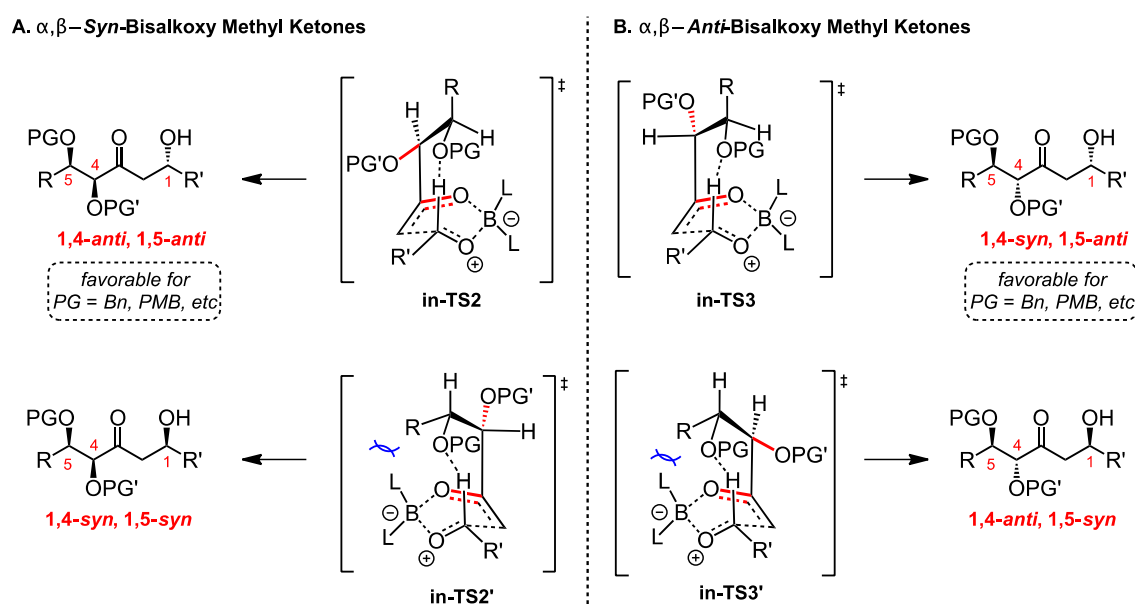


**Figure 8.** Representative calculated transition state geometries for the  $\alpha,\beta$ -*anti*-bisalkoxy methyl ketones.

The most important previous features for  $\alpha,\beta$ -*syn*-bisalkoxy ketones were observed for the  $\alpha,\beta$ -*anti*-bisalkoxy ketones. The analysis of lowest energies **in-TS3** and **in-TS3'** geometries reveals that these transition states also fit with the Goodman-Paton model for 1,5-*anti* selectivity, presenting sta-

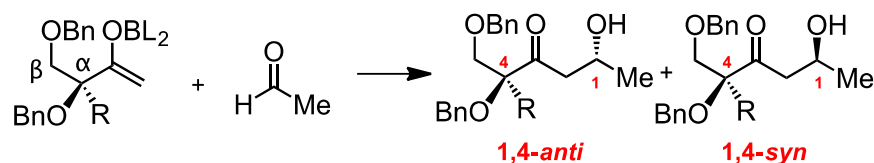
bilizing H-bond (around 4.1 kcal.mol<sup>-1</sup> for 1,5-*anti* and 3.6-4.4 kcal.mol<sup>-1</sup> for 1,5-*syn*), with non-influence of the  $\alpha$ -alkoxy protecting group, and predicting the experimental selectivities in reasonable agreement (Table 3, Figure 8). The origins for the drop of 1,5-*anti* diastereoselectivity for  $\alpha,\beta$ -*anti*-bisalkoxy ketones can be understood considering that the  $\alpha$ -alkoxy center **in-TS3** transition state orientates the C-O bonds of the enolate/ $\alpha$ -alkoxy in a less favorable way in relation to dipole minimization effect. The opposite is expected for **in-TS3'**, helping to stabilize this transition state which would supposedly be responsible for the 1,5-*syn* product and so lead to decrease the 1,5-*anti* experimental diastereoselectivity. The model depicted in Scheme 3 summarizes all previous observations regarding the synergistic effect between the  $\alpha,\beta$ -*syn*-bisalkoxy and  $\alpha,\beta$ -*anti*-bisalkoxy stereocenters.



**Scheme 3:** Proposed induction model for synergistic effect between the  $\alpha,\beta$ -*syn*-bisalkoxy stereocenters in methyl ketones.

Previously, the Goodman-Paton model was used to rationalize the 1,4-*syn* diastereoselectivity of  $\alpha$ -methyl methyl ketones bearing a  $\beta$ -alkoxy group.<sup>6</sup> This diastereoisomeric differentiation originates from the steric interaction between the enolate double bond and the  $\alpha$ -methyl group. A final incursion in our theoretical work regard to investigate the effects of 1,4-induction of  $\alpha$ -alkoxy, $\alpha$ -methyl methyl ketones, as described in Figure 2B. We considered in our calculations two model,  $\alpha,\beta$ -bisalkoxy, $\alpha$ -methyl and  $\alpha,\beta$ -bisalkoxy methyl ketones, as described in Table 4 and Figure 9.

**Table 4.** Relative Gibbs ( $\Delta\Delta G_{rel}$ ) energies (kcal mol<sup>-1</sup>), and theoretical diastereoselectivities for calculated  $\alpha,\beta$ -bisalkoxy methyl ketones.



Enolate	$\Delta\Delta G_{rel}$ (kcal/mol)	$d_{r_{theor}}(1,5\text{-anti}:1,5\text{-syn})^*$ [exp]
R = H	<b>in-TS4</b> <sub>Bn,Bn-a</sub> (1,4- <i>anti</i> )	0.0
	<b>in-TS4'</b> <sub>Bn,Bn-a</sub> (1,4- <i>syn</i> )	2.0
R = Me	<b>in-TS5</b> <sub>Bn,Bn-a</sub> (1,4- <i>anti</i> )	0.0
	<b>in-TS5'</b> <sub>Bn,Bn-a</sub> (1,4- <i>syn</i> )	2.7

\*Determined considering the Boltzmann distribution associated with the Gibbs energies of all observed diastereoisomeric transition states.

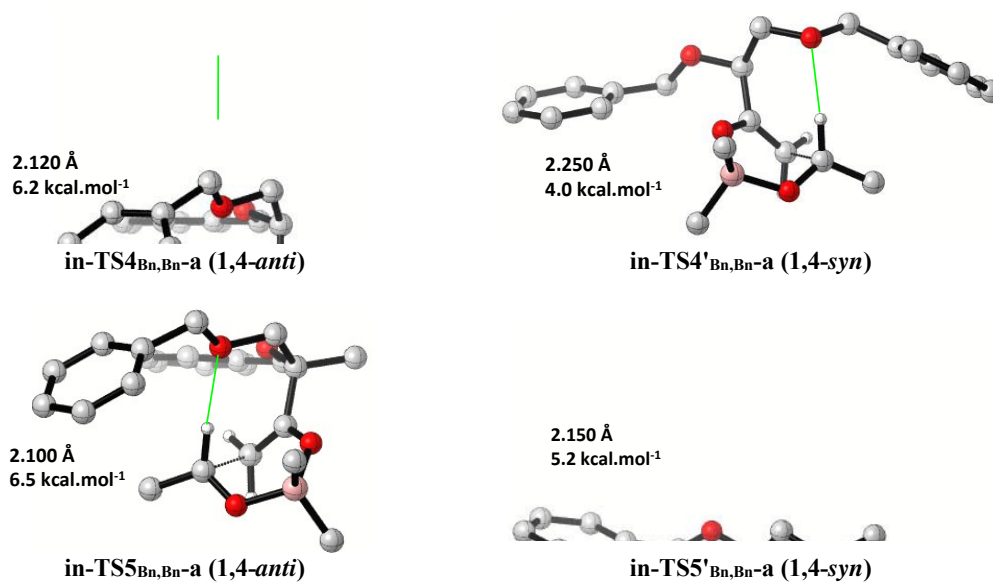
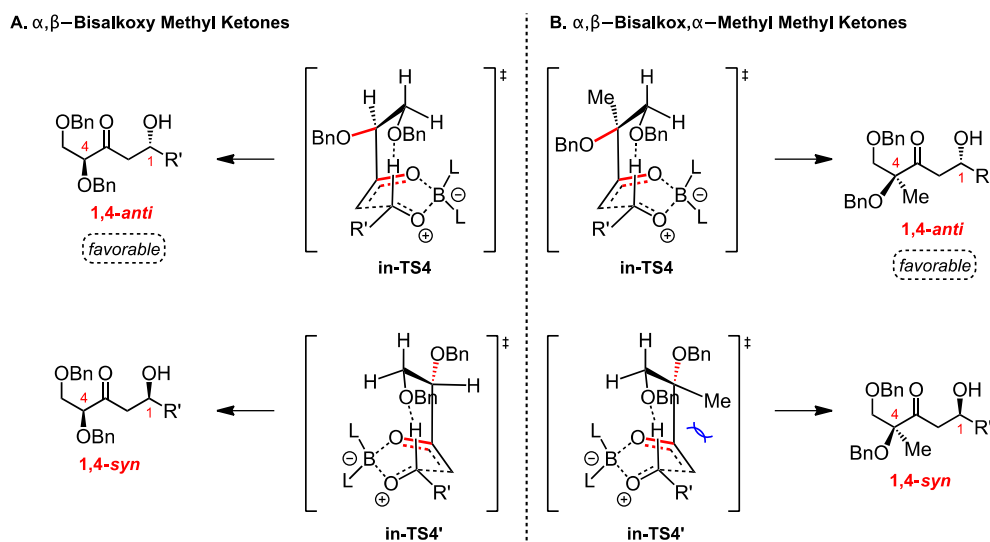


**Figure 9.** Representative calculated transition state geometries for the  $\alpha,\beta$ -bisalkoxy methyl ketones.

In our first model, we excluded the  $\alpha$ -methyl substituent, and the results indicated the prevalence of the Goodman-Paton model to describe the selectivity. The transition states **in-TS4**<sub>Bn,Bn-a</sub> of lowest energies was located predicting the 1,4-*anti* as the major product. This geometry turns of the O-P group eclipsed to the enolate double bond, in order to reduce the dipole of the system, reflecting the dipolar effect discussed before. In the case of  $\alpha,\beta$ -bisalkoxy, $\alpha$ -methyl methyl ketone, the calculations reveal the **in-TS5**<sub>Bn,Bn-a</sub> as the lowest in energy and predicts the 1,4-*anti* as the major diastereoisomer.

As expected, the additional  $\alpha$ -methyl group reinforces the 1,4-*anti* sense of induction with preference for an orthogonal alignment in relation to the enolate double bond, in line with similar transition states reported in literature.<sup>6,22</sup> We conclude that the **in-TS5'**<sub>Bn,Bn-a</sub> is 2.7 kcal mol<sup>-1</sup> higher in energy than **in-TS5**<sub>Bn,Bn-a</sub> due to steric and dipolar reasons. All these observations are depicted in Scheme 4.



**Scheme 4:** Proposed induction model for synergistic effect between the  $\alpha$ -alkoxy,  $\alpha$ -methyl stereocenters in methyl ketones.

## CONCLUSION

In this work, we investigated the 1,4 and 1,5 asymmetric induction presented in boron enolates aldol reactions of  $\alpha$ -alkoxy and  $\alpha,\beta$ -bisalkoxy methyl ketones with commercially available achiral aldehydes. The steric influence of the alkyl substituents at the  $\alpha$  position as well as the stereoelectronic influence of the oxygen protecting groups at the  $\alpha$  and  $\beta$  positions were theoretically and experimentally investigated. Our findings uncover the origins of 1,4 asymmetric induction in terms of the nature of  $\beta$ -substituent. In the presence of the  $\beta$ -alkoxy stereocenter, theoretical calculations help to understand the synergistic effect between the  $\alpha,\beta$ -*syn* and  $\alpha,\beta$ -*anti*-bisalkoxy stereocenters. In these cases, the reaction course goes through the Goodman-Paton 1,5-stereoiduction model, experiencing only a minor influence of the  $\alpha$ -alkoxy group.

## CONFLICTS OF INTEREST

There are no conflicts to declare.

## ACKNOWLEDGEMENTS

Authors acknowledge CNPq, and CAPES for the fellowships conceded. We also gratefully acknowledge financial support from FAPESP (14/50249-8, 15/08541-6) and GlaxoSmithKline (GSK). We are in debit with Prof. Cláudio F. Tormena for computational facilities.

<sup>1</sup> Dias, L. C.; Polo, E. C.; de Lucca, E. C.; Ferreira, M. A. B. (2013) Asymmetric Induction in Aldol Additions, in *Modern Methods in Stereoselective Aldol Reactions* (ed R. Mahrwald), Wiley-VCH Verlag GmbH & Co. KGaA, Weinheim, Germany. (b) Abiko, A. (2016) Boron Enolate Chemistry, Chapter 4, 123-171, ACS Symposium Series, Vol. 1236.

<sup>2</sup> (a) Dias, L. C.; Aguilar, A. M. *Chem. Soc. Rev.* **2008**, *37*, 451. (b) Kan, J.; Ng, K. K.-H.; Paterson, I. *Angew. Chem. Int. Ed.*, **2013**, *52*, 9097. (c) Ferreira, M. A. B.; Dias, L. C.; Leonarczyk, I. A.; Polo, E. C.; Lucca, E. C. *Curr. Org. Syn.* **2015**, *12*, 547. (d) Schetter, B.; Mahrwald, R. *Angew. Chem. Int. Ed.* **2006**, *45*, 7506. (e) Dias, L. C.; Polo, E. C. *J. Org. Chem.* **2017**, *82*, 4072. (f) Dias, L. C.; Lucca, E. C. *J. Org. Chem.* **2017**, *82*, 3019.

<sup>3</sup> For a review covering aldol reactions of  $\alpha$ -hydroxy ketones, see: Aullón, G.; Romea, P.; Urpí, F. *Synthesis* **2017**, *49*, 484.

<sup>4</sup> Rodríguez-Cisterna, V.; Villar, C.; Romea, P.; Urpí, F. *J. Org. Chem.*, **2007**, *72*, 6631.

<sup>5</sup> Goodman, J. M.; Paton, R. S. *Chem. Commun.* **2007**, 2124.

<sup>6</sup> (a) Paton, R. S.; Goodman, J. M. *Org. Lett.* **2006**, *8*, 4299. (b) Paton, R. S.; Goodman, J. M. *J. Org. Chem.* **2008**, *73*, 1253.

<sup>7</sup> Evans, D. A.; Carter, P. H.; Carreira, E. M.; Charette, A. B.; Prunet, J. A.; Lautens, M. *J. Am. Chem. Soc.* **1999**, *121*, 7540.

<sup>8</sup> Fürstner, A.; Kattnig, E.; Lepage, O. *J. Am. Chem. Soc.* **2006**, *128*, 9194.

<sup>9</sup> Lorenz, M.; Bluhm, N.; Kalesse, M. *Synthesis* **2009**, *18*, 3061.

<sup>10</sup> Cowper, N.; Azzi, S.; Dupont-Gaudet, K.; Burch, J. D. *Tetrahedron Lett.* **2012**, *53*, 1837.

<sup>11</sup> (a) Lorente, A.; Pellicena, M.; Romea, P.; Urpí, F. *Tetrahedron Lett.* **2010**, *51*, 942. (b) Lorente, A.; Pellicena, M.; Romea, P.; Urpí, F. *Tetrahedron* **2015**, *71*, 1023. (c) Pellicena, M.; Solsona, J. G.; Romea, P.; Urpí, F. *Tetrahedron Lett.* **2008**, *49*, 5265. (d) Pellicena, M.; Solsona, J. G.; Romea, P.; Urpí, F. *Tetrahedron* **2012**, *68*, 10338.

<sup>12</sup> Gaussian 09, Revision D.01, Frisch, M. J.; Trucks, G. W.; Schlegel, H. B.; Scuseria, G. E.; Robb, M. A.; Cheeseman, J. R.; Scalmani, G.; Barone, V.; Mennucci, B.; Petersson, G. A.; Nakatsuji, H.; Caricato, M.; Li, X.; Hratchian, H. P.; Izmaylov, A. F.; Bloino, J.; Zheng, G.; Sonnenberg, J. L.; Hada, M.; Ehara, M.; Toyota, K.; Fukuda, R.; Hasegawa, J.; Ishida, M.; Nakajima, T.; Honda, Y.; Kitao, O.; Nakai, H.; Vreven, T.; Montgomery, Jr., J. A.; Peralta, J. E.; Ogliaro, F.; Bearpark, M.; Heyd, J. J.; Brothers, E.; Kudin, K. N.; Staroverov, V. N.; Keith, T.; Kobayashi, R.; Normand, J.; Raghavachari, K.; Rendell, A.; Burant, J. C.; Iyengar, S. S.; Tomasi, J.; Cossi, M.; Rega, N.; Millam, J. M.; Klene, M.;

Knox, J. E.; Cross, J. B.; Bakken, V.; Adamo, C.; Jaramillo, J.; Gomperts, R.; Stratmann, R. E.; Yazyev, O.; Austin, A. J.; Cammi, R.; Pomelli, C.; Ochterski, J. W.; Martin, R. L.; Morokuma, K.; Zakrzewski, V. G.; Voth, G. A.; Salvador, P.; Dannenberg, J. J.; Dapprich, S.; Daniels, A. D.; Farkas, O.; Foresman, J. B.; Ortiz, J. V.; Cioslowski, J.; Fox, D. J. Gaussian, Inc., Wallingford CT, **2013**.

<sup>13</sup> (a) Becke, A. D. *Phys. Rev. A*, **1988**, *38*, 3098. b) Perdew, J. P. *Phys. Rev. B*, **1986**, *33*, 8822.

<sup>14</sup> S. Grimme, S. Ehrlich, L. Goerigk *J. Comp. Chem.* **2011**, *32*, 1456.

<sup>15</sup> C. Y. Legault, *CYView. version 1.0b*, Université de Sherbrooke, Canada, 2008.

<sup>16</sup> Glendening, E. D.; Badenhoop, J. K.; Reed, A. E.; Carpenter, J. E.; Bohmann, J. A.; Morales, C. M.; Landis, C. R.; Weinhold, F. (Theoretical Chemistry Institute, University of Wisconsin, Madison, WI, 2013); <http://nbo6.chem.wisc.edu/>

<sup>17</sup> (a) Dias, L. C.; Pinheiro, S. M.; de Oliveira, V. M.; Ferreira, M. A. B.; Tormena, C. F.; Aguilar, A. M.; Zukerman-Schpector, J.; Tiekink, E. R. T. *Tetrahedron* **2009**, *65*, 8714. (b) Dias, L. C.; de Lucca Jr., E. C.; Ferreira, M. A. B.; Garcia, D. C.; Tormena, C. F. *Org. Lett.* **2010**, *21*, 5056. (c) Dias, L. C.; Polo, E. C.; Ferreira, M. A. B.; Tormena, C. F. *J. Org. Chem.* **2012**, *77*, 3766.

<sup>18</sup> Peng, Q.; Duarte, F.; Paton, R. S. *Chem. Soc. Rev.* **2016**, *45*, 6093.

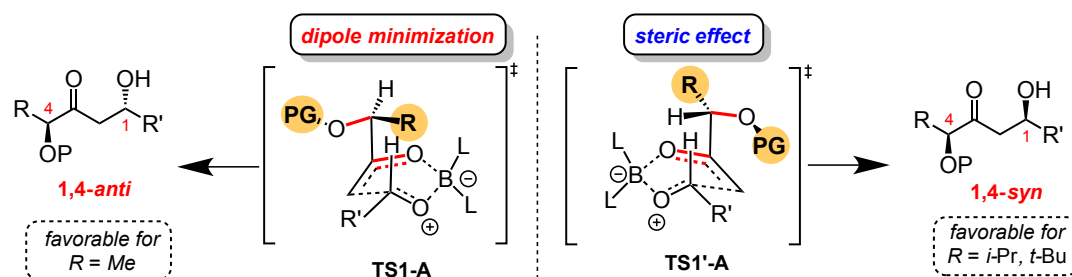
<sup>19</sup> a) Paterson, I.; Gibson, K. R.; Oballa, R. M. *Tetrahedron Lett.* **1996**, *37*, 8585. b) Paterson, I.; Oballa, R. M.; Norcross, R. D. *Tetrahedron Lett.* **1996**, *37*, 8581.

<sup>20</sup> (a) Evans, D. A.; Coleman, P. J.; Côté, B. *J. Org. Chem.* **1997**, *62*, 788. (b) Evans, D. A.; Côté, B.; Coleman, P. J.; Connel, B. T. *J. Am. Chem. Soc.* **2003**, *125*, 10893. (c) Evans, D. A.; Connell, B. T. *J. Am. Chem. Soc.* **2003**, *125*, 10899.

<sup>21</sup> (a) Dias, L. C.; Baú, R. Z.; de Souza, M. A.; Zukerman-Schpector, J. *Org. Lett.* **2002**, *4*, 4325. (b) Dias, L. C.; Aguilar, A. M.; Salles Jr, A. G.; Steil, L. J.; Roush, W. R. *J. Org. Chem.* **2005**, *70*, 10461. (c) Dias, L. C.; Aguilar, A. M. *Org. Lett.* **2006**, *8*, 4629. (d) Dias, L. C.; Salles Jr, A. G. *Tetrahedron Lett.* **2006**, *47*, 2213. (e) Dias, L. C.; de Marchi, A. A.; Ferreira, M. A. B.; Aguilar, A. M. *Org. Lett.* **2007**, *9*, 4869.

<sup>22</sup> If we consider the stereochemistry of  $\alpha$ -methyl stereocenter, the **in-TS**<sub>Bn,Bn</sub>-**a** produce the 1,4-*syn* diastereoisomer, in line with previous results as depicted in reference 6.

## Table of content



PG = protecting group

We investigated the asymmetric induction in boron enolate aldol reactions of  $\alpha$ -alkoxy and  $\alpha,\beta$ -bisalkoxy methyl ketones, and elucidate the synergistic effect between the stereocenters.